Analysis of a Thin Membrane Coated Half-Space under Arbitrary Buried Loads

Hamid Jarfi
Department of Civil Engineering, Sharif University of Technology, P.O. Box 11155-9313, Tehran, Iran
E-mail address: jarfi.hamid@gmail.com

Morteza Eskandari[1]
Department of Civil Engineering, Sharif University of Technology, P.O. Box 11155-9313, Tehran, Iran
Tel.: +98-21-66164275
Fax: +98-21-66072555
Mobile: +98-9373634616
E-mail address: eskandari@sharif.edu

Role of contributors:

Hamid Jarfi: draft preparation, relations derivation, numerical modeling, and data analysis

Morteza Eskandari: original idea, review and interpretation of results, manuscript review

[1] Corresponding author

A brief technical biography of each author:

Hamid Jarfi is currently a Civil Engineering PhD candidate at Sharif University of Technology, Tehran, Iran. He obtained his MSc in Structural Engineering from Sharif University of Technology and has since focused his research on the analytical study of surface effects and thin films using elasticity theories.

Morteza Eskandari is currently an Assistant Professor at School of Civil Engineering at Sharif University of Technology, Tehran, Iran. He has published more than 25 papers in prestigious journals in the area of elasticity. His research interests include wave propagation, mixed-boundary-value problems, and the fracture mechanics of anisotropic solids.

Analysis of a Thin Membrane Coated Half-Space under Arbitrary Buried Loads

H. Jarfi and M. Eskandari*

Abstract

This paper addresses the traditional elasticity problem of a homogeneous isotropic half-space covered by an extremely thin, extensible membrane subjected to arbitrary loads. The membrane, with negligible flexural stiffness, is perfectly attached to the half-space, ensuring continuity of the displacement field. By setting the film thickness to zero and its shear modulus to infinity, equivalent boundary conditions across the thin film surface are derived. Hankel integral transform and Fourier expansion techniques are employed to obtain Muki's potential functions in the transformed domain, yielding a system of equations based on the imposed boundary conditions. Closed-form expressions in the Hankel transformed domain are derived for static problems with general asymmetry. Simplified forms of the proposed boundary conditions are provided for axisymmetric problems. Special cases, including well-known problems such as Kelvin's, Cerruti's, and Mindlin's, are examined for verification purposes. Additionally, a numerical study is conducted to demonstrate the effectiveness of the proposed equations.

Keywords: Thin film, Coated half-space, Transmission condition, Membrane, Geotextile and geo-membrane.

1. Introduction

The use of thin films to enhance the physical and chemical properties of materials is ubiquitous in today's world. Common examples include magnetic thin films for electronic data storage; transparent conductive oxide and absorber layers in solar cells; thin film resistors and dielectrics; catalytic layers for toxic-gas sensing; superconducting thin films for high-frequency devices, data storage, and magnetic circuitry; corrosion-, friction-, and wear-protective layers on automotive and airplane engine parts; and multiple layers on eyeglasses to correct vision, minimize ultraviolet light transmission, and provide scratch resistance [1-3].

Surface-stiffened coatings are added to the media to provide an extra layer of protection from mechanical and environmental conditions. This can greatly improve the performance and extend the working life of the treated parts and components [4,5]. For more examples of this kind of protecting/reinforcing layers in civil engineering constructions, one can find different types of pavement engineering utilizing Carbonphalt or Glasphalt layers [6,7]. The evaluation of existing road pavements is done based on 3 factors: functional surface condition, structural condition, and roughness. Another industrial example is Geomembranes and geotextiles those are being used in environmental, hydraulic, transportation, dam engineering, and oil and gas applications as well as the waste industry [8-11]. Besides, the mechanical properties of the surface of a solid medium or the interface of two bonded media can be different from the bulk properties [12-14]. Therefore, for modelling purposes, such a thin surface layer can be considered as a separate layer with different mechanical properties.

A valuable analytical model to study composite materials is the bi-material full/half-space model; Due to this idea, employing displacement potential methods and integral transforms, Guzina and Pak [15] solved the bi-material full-space under an arbitrary interior point load. A closed-form solution for the elastic fields in two-joined transversely isotropic half-spaces subjected to point force and uniform ring load is presented by Liew et al. [16]. Vijayakumar and Cormack [17] by extending the method of images, established by Mindlin [18] for the first time to obtain a bounded domain solution from an infinite one, provided Green's functions for biharmonic equations especially as to perfectly bonded bi-materials, linear, isotropic, elastic media. The extended Mindlin solution in transversely isotropic half-space with depth heterogeneity expressed in the forms of classical inverse Hankel transform integrals presented by Xiao et al. [19]. For anisotropic bi-materials, Pan and Yuan [20] derived three-dimensional Green's functions based on generalized Stroh formalism and application of the Fourier transform. Green's functions for anisotropic

piezoelectric bi-materials are also presented in a similar manner, by Pan and Yuan [21]. In a dynamic framework, three-dimensional Green's function in transversely isotropic bi-materials was the subject of Khojasteh et al. [22] investigation. An analytical treatment of the response of a transversely isotropic substrate–coating system subjected to axisymmetric time-harmonic excitations presented by Shodja and Eskandari [23]. Analytical solutions for the Rayleigh waves in a piezoelectric semiconductor (PSC) thin film perfectly bonded to an elastic half-space are obtained by Tian et al. [24] and the general solution of each layer is derived by using wave-mode method. Eskandari-Ghadi et al. [25] considered a full space comprised of a transversely isotropic middle layer between two linear elastic half-spaces under an internal load acted on the interface of those of the upper half-space and adjacent layer. Dynamic response of unsaturated full-space caused by a circular tunnel subjected to a vertical harmonic point load analyzed by Song et al. [26]. Similarly, an analytical wave function method for the calculation of vibrations two tunnels embedded in a saturated poroelastic full-space due to a harmonic point load addressed by Yuan et al. [27]. By virtue of a complete set of displacement potential functions and Hankel transform, the Green’s function of an exponentially graded elastic transversely isotropic half-space deriver by Eskandari and Shodja [28]. Oestringer and Proppe [29] presented influence functions for fully coupled quasi-static thermoelastic materials. Those can be used to calculate displacement, stresses as well as temperature distributions within a half-space for arbitrarily shaped heat source or pressure distributions on the surface. The axisymmetric problem of a penny-shaped crack located in a poroelastic half-space solved by Selvadurai and Samea [30]. They also solved the adhesive-impermeable indentation of a poroelastic half-space [31]. An axisymmetric BEM analysis carried out by Xiao and Yue for a one-layered transversely isotropic half-space with cavity [32] as well as for a layered isotropic half-space under internal gas pressure [33].

One of the most important subjects in dealing with bi-materials or generally, composite materials is bonding conditions between two joined surfaces such that associated problems are usually at the forefront of many investigations. Interface crack between two elastic layers is semi-analytically treated by Suo and Hutchinson [34] under fairly general loading conditions. Qu and Bassani [35] focused on aspects of interfacial cracks on anisotropic bi-materials. Selvadurai [36] examined the axisymmetric contact between two smoothly compressed dissimilar elastic half-spaces which is perturbed by a disk inclusion of finite thickness. He, furthermore, evaluated numerically two coupled Fredholm integral equations derived from mixed boundary value-problem and is a consequence of the existence of an embedded inclusion at a bi-material interface [37]. With the aid of Fourier and Abel integral transforms, Gladwell [38] reexamined embedded inclusion at a bi-material interface and provided closed-form expression for the axial stiffness in the states of bonded or partially

bonded contact of rigid circular disk trapped between dissimilar half-spaces. Chen [39] considered the effect of a plane boundary of a piezoelectric body modeled as a thin layer with specified material properties, for which a transfer relation between the state vectors at the top and bottom surfaces is derived based on the state-space formulations. The equations of surface piezoelectricity for different orders without any bias field are then presented by making use of the power series expression of the transfer matrix. In contrast with numerous analytical investigations, fewer researchers focused on experimental observations of bonding conditions in bi-materials; Lambros and Rosakis [40], Wu [41], etc.

Because of its infinitesimal thickness, the bonding zone is often modeled by a thin film, that will affect locally on mechanical boundary conditions, while transmitting from one material to adjacent material. Subsequently, interfacial conditions are called transmission conditions, commonly. Thin films can play various roles in interfacial conditions including inextensible, spring-type, thin or thick plate, and membrane behaviors. Benveniste and Miloh [42] considered a curved isotropic layer of constant thickness, but its properties are varying in the tangential direction, placed between two elastic isotropic media. By assuming a two-dimensional plane-strain state, they introduced seven distinct regimes for interface conditions such as soft and stiff interfaces and so on. Similarly, Benveniste [43] addressed the model of thin interfaces with variable moduli in plane-strain elasticity. An analytical formulation for an axisymmetric response of exponentially graded transversely isotropic tri-material under interfacial loading is presented ye Zafari et al. [44]. Ahmadi et al. [45] obtained the axisymmetric response of bi-material full-space which is reinforced by an interfacial thin film. They presented analytical expressions for special cases such as inextensible thin film and studied surface stiffened half-space as well. Withal transversely bi-material full space strengthened by an inextensible membrane is formulated by Kalantari et al. [46]. With axisymmetric and plane stress considerations, Rahman and Newaz [47] derived the equivalent boundary conditions for an isotopic thin film layer and then solved a semi-infinite isotropic solid whose surface is reinforced by an isotropic thin film and acted upon by an axial ring loading. Thereupon, Ahmadi and Eskandari [48] reduced the mixed boundary value problem of axisymmetric circular indentation of a half-space reinforced by a buried extensible thin film to a Fredholm integral equation of the second kind. This study for an inextensible thin film was achieved by Selvadurai [49]. Eskandari et al. [50] obtained the elastodynamic response of a surface-stiffened transversely isotropic half-space subjected to a buried time-harmonic normal load. Bagheri et al. studied the dispersion of surface waves in transversely isotropic half-space [51].

The current work is associated with discovering and explaining a thin film effect that covers isotropic half-spaces while ensuring perfect boundary

conditions among them. With due attention to the above discussions, it seems investigation of this issue is vital that it can complete previous efforts of researchers. Based on Muki's potential functions, the governing equilibrium equations are rewritten in harmonic and biharmonic equations. With the aid of Fourier expansion and Hankel transform of potential functions and by approaching the thickness of the thin film to zero whereas its shear modulus goes to infinity simultaneously, in section 2, proposed interfacial conditions by Ahmadi et al. [52] are employed and the problem is solved completely. The proposed equivalent surface boundary conditions can be utilized in wide range of research areas such as contact mechanics, different mixed boundary value problems and so on, both in symmetric and asymmetric cases in the context of a half-space. Section 3 is devoted to verification and limiting cases. Furthermore, the effectiveness of proposed transmission conditions is numerically deliberated. Finally, in section 4 concluding remarks are discussed.

2. Problem definition and governing equations

Consider an elastic half-space composed of two dissimilar regions: an elastic thin layer and a lower homogenous half-space. The thin membrane layer and lower half-space are made of homogenous isotropic different materials. The extensible thin membrane of thickness t^F is fully bonded to the lower medium all over. The ascribed system is subjected to an arbitrary static load distributed over an open disc Π_s which is located at the depth *s*. So two regions "I" and "II" in lower half-space for $\left(t^F \le z \le s\right)$ and $\left(z > s\right)$ are recognized, respectively. The origin of the Cartesian coordinates $\left(x_1, x_2, x_3\right)$ and the corresponding cylindrical coordinates $\left(r, \theta, z\right)$ is fixed at the top of the extensible thin membrane.

The elastic constants, shear modulus, and Poisson's ratio of the lower half-space $\left(z > t^F\right)$ will be denoted as μ and ν while those of the thin membrane $\left(0 \le z < t^F\right)$ are denoted as μ^F and ν^F. Hereafter superscript *F* for any given abbreviation represents belonging to the thin film layer, $\left(0 \le z < t^F\right)$.

Because of the thinness of the membrane, its main behavior is in-plane behavior with no flexural stiffness. A tricky strategy to treat the problem has been used. The membrane is considered an elastic layer with a thickness of t^F covering a half-space; This composite elasticity problem has been approached by the use of potential functions up to the point where boundary conditions are applied. At this final stage, the main idea is implemented by taking limits of the thin membrane layer.

In cylindrical coordinates the static equations of equilibrium for any elastic layer in the absence of body forces are [53]:

$$\frac{\partial \sigma_{rr}}{\partial r}+\frac{\sigma_{rr}-\sigma_{\theta\theta}}{r}+\frac{1}{r}\frac{\partial \sigma_{r\theta}}{\partial \theta}+\frac{\partial \sigma_{rz}}{\partial z}=0, \tag{1a}$$

$$\frac{\partial \sigma_{r\theta}}{\partial r}+2\frac{\sigma_{r\theta}}{r}+\frac{1}{r}\frac{\partial \sigma_{\theta\theta}}{\partial \theta}+\frac{\partial \sigma_{\theta z}}{\partial z}=0, \tag{1b}$$

$$\frac{\partial \sigma_{rz}}{\partial r}+\frac{\sigma_{r\theta}}{r}+\frac{1}{r}\frac{\partial \sigma_{z\theta}}{\partial \theta}+\frac{\partial \sigma_{zz}}{\partial z}=0, \tag{1c}$$

in which the stress components, σ_{ij}, are related to strain components, ε_{ij}, as:

$$\sigma_{rr}=\lambda\left(\varepsilon_{rr}+\varepsilon_{\theta\theta}+\varepsilon_{zz}\right)+2\mu\varepsilon_{rr}, \tag{2a}$$

$$\sigma_{\theta\theta}=\lambda\left(\varepsilon_{rr}+\varepsilon_{\theta\theta}+\varepsilon_{zz}\right)+2\mu\varepsilon_{\theta\theta}, \tag{2b}$$

$$\sigma_{zz}=\lambda\left(\varepsilon_{rr}+\varepsilon_{\theta\theta}+\varepsilon_{zz}\right)+2\mu\varepsilon_{zz}, \tag{2c}$$

$$\sigma_{r\theta}=\mu\varepsilon_{r\theta}, \qquad \sigma_{z\theta}=\mu\varepsilon_{z\theta}, \qquad \sigma_{rz}=\mu\varepsilon_{rz}, \tag{2d}$$

where λ and μ are Lamé constants. The strain components are achieved from displacement field components, u_r, u_θ and u_z which are in $r, \theta,$ and z directions, respectively.

$$\varepsilon_{rr}=\frac{\partial u_r}{\partial r}, \qquad \varepsilon_{\theta\theta}=\frac{1}{r}\left(\frac{\partial u_\theta}{\partial \theta}+u_r\right), \tag{3a}$$

$$\varepsilon_{rr}=\frac{\partial u_z}{\partial z}, \qquad \varepsilon_{r\theta}=\frac{1}{r}\frac{\partial u_r}{\partial \theta}+r\frac{\partial}{\partial r}\left(\frac{u_\theta}{r}\right), \tag{3b}$$

$$\varepsilon_{z\theta}=\frac{1}{r}\frac{\partial u_z}{\partial \theta}+\frac{\partial u_\theta}{\partial z}, \qquad \varepsilon_{rz}=\frac{\partial u_r}{\partial z}+\frac{\partial u_z}{\partial r}. \tag{3c}$$

By combining the Eqs. (2) and (3), the equilibrium equation (1), can be expressed in the well-known Cauchy-Navier equations in terms of displacement components as follow:

$$\left(\lambda+\mu\right)\frac{\partial}{\partial r}\left(\frac{1}{r}\frac{\partial\left(ru_r\right)}{\partial r}+\frac{1}{r}\frac{\partial u_\theta}{\partial \theta}+\frac{\partial u_z}{\partial z}\right)+\mu\left(\nabla^2 u_r-\frac{u_r}{r^2}-\frac{2}{r^2}\frac{\partial u_\theta}{\partial \theta}\right)=0, \tag{4a}$$

$$\left(\lambda+\mu\right)\frac{\partial}{r\partial \theta}\left(\frac{1}{r}\frac{\partial\left(ru_r\right)}{\partial r}+\frac{1}{r}\frac{\partial u_\theta}{\partial \theta}+\frac{\partial u_z}{\partial z}\right)+\mu\left(\nabla^2 u_\theta-\frac{u_\theta}{r^2}+\frac{2}{r^2}\frac{\partial u_r}{\partial \theta}\right)=0, \tag{4b}$$

$$\left(\lambda+\mu\right)\frac{\partial}{\partial z}\left(\frac{1}{r}\frac{\partial\left(ru_r\right)}{\partial r}+\frac{1}{r}\frac{\partial u_\theta}{\partial \theta}+\frac{\partial u_z}{\partial z}\right)+\mu\nabla^2 u_z=0, \tag{4c}$$

where Laplace operator, ∇^2, in the cylindrical coordinate system is defined as $\nabla^2 = \frac{\partial^2}{\partial r^2} + \frac{1}{r}\frac{\partial}{\partial r} + \frac{1}{r^2}\frac{\partial^2}{\partial \theta^2} + \frac{\partial^2}{\partial z^2}$. Generally, in asymmetric problems Muki's potential functions ϕ and ψ may be used [54], which leads to reduction of the Cauchy-Navier equations to the following partial differential equations:

$$\nabla^2 \psi = 0, \tag{5a}$$

$$\nabla^2 \nabla^2 \phi = 0. \tag{5b}$$

The displacement components in terms of above-mentioned functions are given as:

$$u_r = \frac{1}{2\mu}\left(-\frac{\partial^2 \phi}{\partial r \partial z} + \frac{2}{r}\frac{\partial \psi}{\partial \theta} \right), \tag{6a}$$

$$u_\theta = \frac{1}{2\mu}\left(-\frac{1}{r}\frac{\partial^2 \phi}{\partial \theta\, \partial z} - \frac{\partial \psi}{\partial r} \right), \tag{6b}$$

$$u_z = \frac{1}{2\mu}\left(2(1-\nu)\nabla^2 \phi - \frac{\partial^2 \phi}{\partial z^2} \right), \tag{6c}$$

and through using Eqs. (2) and (3), stress components are given as follow, simply:

$$\sigma_{rr} = \frac{\partial}{\partial z}\left(\nu \nabla^2 - \frac{\partial^2}{\partial r^2} \right)\phi + \frac{\partial}{\partial \theta}\left(\frac{2}{r}\frac{\partial}{\partial r} - \frac{2}{r^2} \right)\psi, \tag{7a}$$

$$\sigma_{\theta\theta} = \frac{\partial}{\partial z}\left(\nu \nabla^2 - \frac{1}{r}\frac{\partial}{\partial r} - \frac{1}{r^2}\frac{\partial^2}{\partial \theta^2} \right)\phi - \frac{\partial}{\partial \theta}\left(\frac{2}{r}\frac{\partial}{\partial r} - \frac{2}{r^2} \right)\psi, \tag{7b}$$

$$\sigma_{zz} = \frac{\partial}{\partial z}\left((2-\nu)\nabla^2 - \frac{\partial^2}{\partial z^2} \right)\phi, \tag{7c}$$

$$\sigma_{\theta z} = \frac{1}{r}\frac{\partial}{\partial \theta}\left((1-\nu)\nabla^2 - \frac{\partial^2}{\partial z^2} \right)\phi - \frac{\partial^2}{\partial r \partial z}\psi, \tag{7d}$$

$$\sigma_{zr} = \frac{\partial}{\partial r}\left((1-\nu)\nabla^2 - \frac{\partial^2}{\partial z^2} \right)\phi + \frac{1}{r}\frac{\partial^2}{\partial \theta \partial z}\psi, \tag{7e}$$

$$\sigma_{r\theta} = \frac{1}{r}\frac{\partial^2}{\partial \theta \partial z}\left(\frac{1}{r} - \frac{\partial}{\partial r} \right)\phi - \left(\frac{\partial^2}{\partial r^2} - \frac{1}{r}\frac{\partial}{\partial r} - \frac{1}{r^2}\frac{\partial^2}{\partial \theta^2} \right)\psi, \tag{7f}$$

in all of which ν is Poisson's ratio. With regard to the completeness of the set of angular eigenfunctions, $e^{im\theta}$, stress functions ϕ and ψ can be expressed in the harmonic form of angular coordinate, θ in a proper form for odd or even functions:

$$\left\{\phi(r,\theta,z),\quad \psi(r,\theta,z)\right\}=\sum_{m=-\infty}^{+\infty}\left\{\phi_m(r,z),\quad \psi_m(r,z)\right\}e^{im\theta}, \tag{8a}$$

$$\left\{\phi_m(r,z),\quad \psi_m(r,z)\right\}=\frac{1}{2\pi}\int_0^{2\pi}\left\{\phi(r,\theta,z),\quad \psi(r,\theta,z)\right\}e^{im\theta}d\theta. \tag{8b}$$

By using Fourier expansion, Eq. (5) results in

$$\left(\frac{\partial^2}{\partial r^2}+\frac{1}{r}\frac{\partial}{\partial r}-\frac{m^2}{r^2}+\frac{\partial^2}{\partial z^2}\right)\psi_m=0, \tag{9a}$$

$$\left(\frac{\partial^2}{\partial r^2}+\frac{1}{r}\frac{\partial}{\partial r}-\frac{m^2}{r^2}+\frac{\partial^2}{\partial z^2}\right)^2\phi_m=0. \tag{9b}$$

To solve these partial differential equations, it is convenient to introduce the m^{th}-order Hankel transform of function $f(r,z)$ and its inversion, respectively, as follows:

$$\tilde{f}^m(\xi,z)=\int_0^\infty rf(r,z)J_m(r\xi)dr, \tag{10a}$$

$$f(r,z)=\int_0^\infty \xi f(\xi,z)J_m(r\xi)d\xi, \tag{10b}$$

where $\tilde{f}^m(\xi,z)$ shows the corresponding function of $f(r,z)$ in the Hankel transformed domain; ξ is the Hankel transform parameter with respect to radial coordinate and J_m denotes the m^{th}-order Bessel function of the first kind. Application of this integral transform on Eq. (9) yields:

$$\left(-\xi^2+\frac{d^2}{dz^2}\right)\tilde{\psi}_m^m=0, \tag{11a}$$

$$\left(-\xi^2+\frac{d^2}{dz^2}\right)^2\tilde{\phi}_m^m=0. \tag{11b}$$

Here $\tilde{\phi}_m^m(\xi,z)$ and $\tilde{\psi}_m^m(\xi,z)$ are the m^{th}-order Hankel transformed functions of the corresponding mth term in Fourier expansion of potential functions $\phi_m(r,z)$ and $\psi_m(r,z)$, respectively. With due attention to the regularity conditions at infinity (i.e. vanishing elastic fields for $\sqrt{r^2+z^2}\to\infty$), the above

set of ordinary differential Eq. (11) reaches the following expressions for potential functions for each region:

$$\tilde{\psi}_m^{mF}(\xi,z)=a^F e^{-\xi z}+b^F e^{\xi z}, \tag{12a}$$

$$\tilde{\phi}_m^{mF}(\xi,z)=\left(c^F+d^F z\right)e^{-\xi z}+\left(f^F+g^F z\right)e^{\xi z}, \tag{12b}$$

$$\tilde{\psi}_m^{mI}(\xi,z)=a^I e^{-\xi z}+b^I e^{\xi z}, \tag{12c}$$

$$\tilde{\phi}_m^{mI}(\xi,z)=\left(c^I+d^I z\right)e^{-\xi z}+\left(f^I+g^I z\right)e^{\xi z}, \tag{12d}$$

$$\tilde{\psi}_m^{mII}(\xi,z)=a^{II} e^{-\xi z}, \tag{12e}$$

$$\tilde{\phi}_m^{mII}(\xi,z)=\left(c^{II}+d^{II} z\right)e^{-\xi z}, \tag{12f}$$

where $\left\{a^\alpha,b^\alpha,c^\alpha,d^\alpha,f^\alpha,g^\alpha\right\},(\alpha=I,II,F)$ are fifteen unknown constants to be determined by satisfying the following boundary conditions at all interfaces such a way that continuity for displacements across each interface plane is preserved

$$\sigma_{zz}^F=0,\quad \sigma_{rz}^F=0,\quad \sigma_{\theta z}^F=0,\quad at\ z=0 \tag{13a}$$

$$u_z^F=u_z^I,\quad u_r^F=u_r^I,\quad u_\theta^F=u_\theta^I,\quad at\ z=t^F \tag{13b}$$

$$\sigma_{zz}^F=\sigma_{zz}^I,\quad \sigma_{zr}^F=\sigma_{zr}^I,\quad \sigma_{z\theta}^F=\sigma_{z\theta}^I,\quad at\ z=t^F \tag{13c}$$

$$u_z^I=u_z^{II},\quad u_r^I=u_r^{II},\quad u_\theta^I=u_\theta^{II},\quad at\ z=s. \tag{13d}$$

The distributed body-force field as a general discontinuity in stresses over Π_s across the plane $z=s$ is defined as

$$\sigma_{zr}\left(r,\theta,s^-\right)-\sigma_{zr}\left(r,\theta,s^+\right)=\begin{cases}P(r,\theta), & (r,\theta,s)\in\Pi_s\\ 0\quad , & (r,\theta,s)\notin\Pi_s\end{cases}, \tag{14a}$$

$$\sigma_{z\theta}\left(r,\theta,s^-\right)-\sigma_{z\theta}\left(r,\theta,s^+\right)=\begin{cases}Q(r,\theta), & (r,\theta,s)\in\Pi_s\\ 0\quad , & (r,\theta,s)\notin\Pi_s\end{cases}, \tag{14b}$$

$$\sigma_{zz}\left(r,\theta,s^-\right)-\sigma_{zz}\left(r,\theta,s^+\right)=\begin{cases}R(r,\theta), & (r,\theta,s)\in\Pi_s\\ 0\quad , & (r,\theta,s)\notin\Pi_s\end{cases}, \tag{14c}$$

where $P(r,\theta)$, $Q(r,\theta)$, and $R(r,\theta)$ are components of asymmetric forces in the radial, angular, and axial directions, respectively. To impose perfect adhering assumption between the thin film and its lower half-space, and also other boundary conditions, Eqs. (13) and (14) should be developed in Hankel transformed domain concerning the same radial component of cylindrical coordinate, r. The m^{th}-order Hankel transform of the displacement field leads to the following relations, [52]:

$$2\mu\tilde{u}_{z_m}^{m}=\left(-2(1-\nu)\xi^{2}+(1-2\nu)\frac{\partial^{2}}{\partial z^{2}}\right)\tilde{\phi}_{m}^{m}, \tag{15a}$$

$$2\mu\left(\tilde{u}_{r_m}^{m+1}+i\tilde{u}_{\theta_m}^{m+1}\right)=\xi\frac{\partial\tilde{\phi}_{m}^{m}}{\partial z}+2i\xi\tilde{\psi}_{m}^{m}, \tag{15b}$$

$$2\mu\left(\tilde{u}_{r_m}^{m-1}-i\tilde{u}_{\theta_m}^{m-1}\right)=-\xi\frac{\partial\tilde{\phi}_{m}^{m}}{\partial z}+2i\xi\tilde{\psi}_{m}^{m}, \tag{15c}$$

$$\tilde{\sigma}_{rr_m}^{m}+2\mu\left(\left(\frac{\tilde{u}_{r_m}}{r}\right)^{m}+im\left(\frac{\tilde{u}_{\theta_m}}{r}\right)^{m}\right)=\frac{\partial}{\partial z}\left((1-\nu)\xi^{2}+\nu\frac{\partial^{2}}{\partial z^{2}}\right)\tilde{\phi}_{m}^{m}, \tag{15d}$$

$$\tilde{\sigma}_{\theta\theta_m}^{m}-2\mu\left(\left(\frac{\tilde{u}_{r_m}}{r}\right)^{m}+im\left(\frac{\tilde{u}_{\theta_m}}{r}\right)^{m}\right)=\frac{\partial}{\partial z}\left(-\nu\xi^{2}+\nu\frac{\partial^{2}}{\partial z^{2}}\right)\tilde{\phi}_{m}^{m}, \tag{15e}$$

$$\tilde{\sigma}_{zz_m}^{m}=\frac{\partial}{\partial z}\left(-(2-\nu)\xi^{2}+(1-\nu)\frac{\partial^{2}}{\partial z^{2}}\right)\tilde{\phi}_{m}^{m}, \tag{15f}$$

$$\tilde{\sigma}_{rz_m}^{m+1}+i\tilde{\sigma}_{\theta z_m}^{m+1}=\xi\left((1-\nu)\xi^{2}+\nu\frac{\partial^{2}}{\partial z^{2}}\right)\tilde{\phi}_{m}^{m}+i\xi\frac{\partial}{\partial z}\tilde{\psi}_{m}^{m}, \tag{15g}$$

$$\tilde{\sigma}_{rz_m}^{m-1}-i\tilde{\sigma}_{\theta z_m}^{m-1}=-\xi\left((1-\nu)\xi^{2}+\nu\frac{\partial^{2}}{\partial z^{2}}\right)\tilde{\phi}_{m}^{m}+i\xi\frac{\partial}{\partial z}\tilde{\psi}_{m}^{m}, \tag{15h}$$

$$\tilde{\sigma}_{r\theta_m}^{m}-2\mu\left(im\left(\frac{\tilde{u}_{r_m}}{r}\right)^{m}-\left(\frac{\tilde{u}_{\theta_m}}{r}\right)^{m}\right)=\xi^{2}\tilde{\psi}_{m}^{m}. \tag{15i}$$

Substitution of potential functions shown in expressions (12) in boundary conditions (13) and (14), by virtue of Eq. (15) results in a system of 15 equations with 15 unknown coefficients. Usually, the inversion of the coefficient matrix has to be found to determine potential functions, $\tilde{\phi}_{m}^{m}$ and $\tilde{\psi}_{m}^{m}$ with respect to the integral transform parameter, ξ. The application of inverse Hankel transform in relations $\tilde{\phi}_{m}^{m}$ and $\tilde{\psi}_{m}^{m}$ leads to inexplicable results whereas the procedure itself is exhausting. Here, a simple yet useful method for surface conditions is proposed by Ahmadi et al. [52] in a way that by removal of thin film, its impact is remained by tending t^{F} to zero and simultaneously tending μ^{F} to infinity such that $\kappa=2\left(1+\nu^{F}\right)\mu^{F}t^{F}$ (henceforth called rigidity) remains fixed. Under plane stress considerations and by introducing hereunder functions in the transformed domain:

$$\tilde{\Pi}_m^m = 2\xi\left(\left(1-\nu\right)\xi^2 + \nu\frac{\partial^2}{\partial z^2}\right)\tilde{\phi}_m^m, \tag{16a}$$

$$\tilde{\Omega}_m^m = 2i\xi\frac{\partial}{\partial z}\tilde{\psi}_m^m, \tag{16b}$$

$$\tilde{\Gamma}_m^m = \frac{\xi}{\mu}\frac{\partial\tilde{\phi}_m^m}{\partial z}, \tag{16c}$$

$$\tilde{\Lambda}_m^m = 2i\frac{\xi}{\mu}\tilde{\psi}_m^m. \tag{16d}$$

Their proposed equivalent conditions yield

$$\left(\frac{\kappa}{2\left(1+\nu^F\right)}\xi^2 - \mu\frac{\partial}{\partial z}\right)\tilde{\psi}_m^{m^I} = 0, \tag{17}$$

$$\left(\nu\frac{\partial^2}{\partial z^2} - \frac{\kappa\xi^2}{2\mu\left(1+\nu^F\right)\left(1-\nu^F\right)}\frac{\partial}{\partial z} + \left(1-\nu\right)\xi^2\right)\tilde{\phi}_m^m = 0, \tag{18}$$

as thin film treatment on the surface of a half-space. According to the new introduced approach, by utilizing Eqs. (17) and (18) the shear stresses transmission conditions at the same depth at which the thin film is located, here at the surface of half-space $z=0$, links to in-plane deformations thoughtfully whilst normal stresses transmit without any disturbance across thin film (for more demonstrations, please refer to [52]):

$$\frac{\partial}{\partial z}\left(-\left(2-\nu\right)\xi^2 + \left(1-\nu\right)\frac{\partial^2}{\partial z^2}\right)\tilde{\phi}_m^{m^I} = 0. \tag{19}$$

These equations can be used to address various contact mechanics and mixed boundary value problems. Additionally, by removing the thin film, the proposed surface conditions simplify the solving process by reducing unknown constants and ensuring proper convergence of all inverse integrals.

Relations (17)-(19) in addition to six relations at depth $z=s$, Eqs. (13) and (14), provide enough equations to solve 9 unknowns easily. Substitution of the result into Eq. (15) gives the transformed Fourier components of the displacements:

$$\tilde{u}_{r_m}^{m-1} - i\tilde{u}_{\theta_m}^{m-1} = \gamma_1\left(\xi,z;s\right)\left(\frac{X_m - Y_m}{2\mu}\right) + \gamma_2\left(\xi,z;s\right)\left(\frac{X_m + Y_m}{2\mu}\right) + \gamma_3\left(\xi,z;s\right)\left(\frac{Z_m}{\mu}\right),$$

$$\tilde{u}_{r_m}^{m+1} + i\tilde{u}_{\theta_m}^{m+1} = -\gamma_1\left(\xi,z;s\right)\left(\frac{X_m - Y_m}{2\mu}\right) + \gamma_2\left(\xi,z;s\right)\left(\frac{X_m + Y_m}{2\mu}\right) - \gamma_3\left(\xi,z;s\right)\left(\frac{Z_m}{\mu}\right),$$

$$\tilde{u}_{z_m}^m = \Omega_1(\xi, z; s)\left(\frac{X_m - Y_m}{2\mu}\right) + \Omega_2(\xi, z; s)\left(\frac{Z_m}{\mu}\right), \tag{20}$$

where the kernel functions γ_1, γ_2, γ_3, Ω_1, and Ω_2 are as follow

$$\gamma_1(\xi, z; s) = \frac{1}{I(\xi)}\left\{\kappa\xi(1-\nu)\left[-\alpha^- e^{-(s+z)\xi} + \beta^- e^{-|z-s|\xi}\right]\right.$$
$$\left. + \mu\left(1-\nu^{F^2}\right)\left[\left(5-12\nu+8\nu^2-(3-4\nu)\xi(s+z)+2sz\xi^2\right)e^{-(s+z)\xi} + \beta^- e^{-|z-s|\xi}\right]\right\},$$

$$\gamma_2(\xi, z; s) = \frac{2\mu\left(1+\nu^F\right)\left[e^{-(s+z)\xi} + e^{-|z-s|\xi}\right] - \kappa\xi\left[e^{-(s+z)\xi} - e^{-|z-s|\xi}\right]}{2\xi\left[2\mu\left(1+\nu^F\right) + \kappa\xi\right]},$$

$$\gamma_3(\xi, z; s) = \frac{1}{I(\xi)}\left\{\kappa\xi^2(1-\nu)\left[-(s+z)e^{-(s+z)\xi} + (s-z)e^{-|z-s|\xi}\right]\right.$$
$$\left. + \mu\left(1-\nu^{F^2}\right)\left[\left(4-12\nu+8\nu^2+(3-4\nu)\xi(s-z)-2sz\xi^2\right)e^{-(s+z)\xi} + (s-z)e^{-|z-s|\xi}\right]\right\},$$

$$\Omega_1(\xi, z; s) = \frac{1}{I(\xi)}\left\{\kappa\xi^2(1-\nu)\left[-(s+z)e^{-(s+z)\xi} - (s-z)e^{-|z-s|\xi}\right]\right.$$
$$\left. + \mu\left(1-\nu^{F^2}\right)\left[\left(4-12\nu+8\nu^2+(3-4\nu)\xi(z-s)-2sz\xi^2\right)e^{-(s+z)\xi} + (z-s)e^{-|z-s|\xi}\right]\right\},$$

$$\Omega_2(\xi, z; s) = \frac{1}{I(\xi)}\left\{\kappa\xi(1-\nu)\left[\alpha^+ e^{-(s+z)\xi} + \beta^+ e^{-|z-s|\xi}\right]\right.$$
$$\left. + \mu\left(1-\nu^{F^2}\right)\left[\left(5-12\nu+8\nu^2+(3-4\nu)\xi(s+z)+2sz\xi^2\right)e^{-(s+z)\xi} + \beta^+ e^{-|z-s|\xi}\right]\right\}, \tag{21}$$

Here

$$X_m = \tilde{P}_m^{m-1}(\xi) - i\tilde{Q}_m^{m-1}(\xi),$$
$$Y_m = \tilde{P}_m^{m+1}(\xi) + i\tilde{Q}_m^{m+1}(\xi),$$
$$\tilde{Z}_m^m = \tilde{R}_m^m(\xi),$$
$$\alpha^{\pm}(\xi, z; s) = 3-4\nu \pm \xi(s+z),$$
$$\beta^{\pm}(\xi, z; s) = 3-4\nu \pm \xi|z-s|,$$
$$I(\xi) = 8\xi(1-\nu)\left[\mu\left(1-\nu^{F^2}\right) + \kappa\xi(1-\nu)\right]. \tag{22}$$

As well as, the corresponding stress field yields

$$\tilde{\sigma}_{zz_m}^{m}=\left(\frac{d\Omega_1}{dz}+2\xi\gamma_1-\frac{\nu}{\xi}\frac{d^2\gamma_1}{dz^2}\right)\left(\frac{X_m-Y_m}{2}\right)+\left(\frac{d\Omega_2}{dz}+2\xi\gamma_3-\frac{\nu}{\xi}\frac{d^2\gamma_3}{dz^2}\right)Z_m,$$

$$\tilde{\sigma}_{rz_m}^{m+1}+i\tilde{\sigma}_{\theta z_m}^{m+1}=-\left(\xi\Omega_1+\frac{d\gamma_1}{dz}\right)\frac{X_m-Y_m}{2}+\frac{d\gamma_2}{dz}\frac{X_m+Y_m}{2}-\left(\xi\Omega_2+\frac{d\gamma_3}{dz}\right)Z_m, \qquad (23)$$

$$\tilde{\sigma}_{rz_m}^{m+1}+i\tilde{\sigma}_{\theta z_m}^{m+1}=\left(\xi\Omega_1+\frac{d\gamma_1}{dz}\right)\frac{X_m-Y_m}{2}+\frac{d\gamma_2}{dz}\frac{X_m+Y_m}{2}+\left(\xi\Omega_2+\frac{d\gamma_3}{dz}\right)Z_m.$$

After substituting the inverted Fourier components of the displacement into the corresponding angular eigenfunction expansions, the desired formal solution to the general buried source problem can be obtained.

3. Special cases and verification

So as to verify the utilized approach for modeling a thin membrane and evaluate the accuracy of presented results, several particular cases including the axisymmetric loads, unreinforced half-space and inextensible thin film reinforced half-space are studied and addressed in the literature, [15].

3.1. Axisymmetric loading problem

In the case of axial symmetrical loads, it can be seen clearly that Eq. (17) becomes trivial relation; On the other hand, the equation of Eq. (18) with $m=0$ reduces to

$$\tilde{\sigma}_{rz_0}^{1}\left(\xi,0\right)-\tilde{\sigma}_{rz_0}^{-1}\left(\xi,t^F\right)=\frac{2\mu^F t^F}{1-\nu^F}\xi^2\left(\tilde{u}_{r_0}^{1}-\tilde{u}_{r_0}^{-1}\right), \qquad (24)$$

which is a transformed form of relation:

$$\sigma_{rz}\left(r,0\right)-\sigma_{rz}\left(r,t^F\right)=\frac{2\mu^F t^F}{1-\nu^F}\left(\frac{d^2u_r^*}{dr^2}+\frac{1}{r}\frac{du_r^*}{dr}-\frac{u_r^*}{r^2}\right), \qquad (25)$$

mentioned by M. Rahman and G. Newaz [47] previously for thin films with generalized plane stress consideration.

Due to axial symmetry of this case, $\sigma_{z\theta}\left(r,\theta,z\right)=u_\theta\left(r,\theta,z\right)=0$, and other displacement and stress field components simplified as:

$$\left\{u_r\left(r,z\right),\quad u_z\left(r,z\right)\right\}=\int_0^\infty\left\{\Omega_1^{axi}J_1\left(r\xi\right),\quad \Omega_2^{axi}J_0\left(r\xi\right)\right\}\tilde{R}_0^0\xi d\xi,$$

$$\left\{\sigma_{rz}\left(r,z\right),\quad \sigma_{zz}\left(r,z\right)\right\}=\int_0^\infty\left\{\Omega_3^{axi}J_1\left(r\xi\right),\quad \Omega_4^{axi}J_0\left(r\xi\right)\right\}\tilde{R}_0^0\xi d\xi, \qquad (26)$$

and the kernel functions, $\Omega_i^{axi}\left(i=1,\ 2,\ 3,\ 4\right)$ are obtained as

$$\Omega_1^{axi}\left(\xi,z;s\right)=\frac{1}{I\left(\xi\right)\mu}\left\{\kappa\xi^2\left(1-\nu\right)\left[\left(s+z\right)e^{-\left(s+z\right)\xi}-\left(s-z\right)e^{-\left|z-s\right|\xi}\right]\right.$$
$$\left.-\mu\left(1-\nu^{F^2}\right)\left[\left(s-z\right)\xi e^{-\left|z-s\right|\xi}+\left(4-4\nu\left(3-2\nu\right)+\left(3-4\nu\right)\xi\left(s-z\right)-2sz\xi^2\right)e^{-\left(s+z\right)\xi}\right]\right\},$$

$$\Omega_2^{axi}\left(\xi,z;s\right)=\frac{1}{I\left(\xi\right)\mu}\left\{\kappa\xi\left(1-\nu\right)\left[\left(3-4\nu+\xi\left(s+z\right)\right)e^{-\left(s+z\right)\xi}+\left(3-4\nu+\xi\left|z-s\right|\right)e^{-\left|z-s\right|\xi}\right]\right.$$
$$\left.+\mu\left(1-\nu^{F^2}\right)\left[\left(3-4\nu+\xi\left|z-s\right|\right)e^{-\left|z-s\right|\xi}+\left(5-4\nu\left(3-2\nu\right)+\left(3-4\nu\right)\xi\left(s+z\right)+2sz\xi^2\right)e^{-\left(s+z\right)\xi}\right]\right\},$$

$$\Omega_3^{axi}\left(\xi,z;s\right)=-\frac{2\xi}{I\left(\xi\right)}\left\{\kappa\xi\left(1-\nu\right)\left[\left(1-2\nu+\xi\left(s+z\right)\right)e^{-\left(s+z\right)\xi}+\left(1-2\nu+\xi\left|z-s\right|\right)e^{-\left|z-s\right|\xi}\right]\right.$$
$$\left.-\mu\left(1-\nu^{F^2}\right)\left[\left(1-2\nu+s\xi-\left(3-4\nu\right)z\xi-2sz\xi^2\right)e^{-\left(s+z\right)\xi}-\left(1-2\nu+\xi\left|s-z\right|\right)e^{-\left|z-s\right|\xi}\right]\right\},$$

$$\Omega_4^{axi}\left(\xi,z;s\right)=-\frac{2\xi}{I\left(\xi\right)}\left\{\kappa\xi\left(1-\nu\right)\left[\left(2-2\nu+\xi\left(s+z\right)\right)e^{-\left(s+z\right)\xi}-\left(2-2\nu+\xi\left|z-s\right|\right)e^{-\left|z-s\right|\xi}\right]\right.$$
$$\left.+\mu\left(1-\nu^{F^2}\right)\left[\left(2-2\nu+s\xi+\left(3-4\nu\right)z\xi+2sz\xi^2\right)e^{-\left(s+z\right)\xi}-\left(2-2\nu+\xi\left|z-s\right|\right)e^{-\left|z-s\right|\xi}\right]\right\},\qquad(27)$$

and definition of $I\left(\xi\right)$ in relation (22) is hold.

3.2. Unreinforced half-space

For the limiting case of $\kappa\to 0$, the solution corresponding to a half-space under an arbitrary buried loading is obtained:

$$\gamma_1^{hs}\left(\xi,z;s\right)=\frac{1}{8\xi\left(1-\nu\right)}\left[\left(5-12\nu+8\nu^2-\left(3-4\nu\right)\xi\left(s+z\right)+2sz\xi^2\right)e^{-\left(s+z\right)\xi}+\left(3-4\nu-\left|z-s\right|\xi\right)e^{-\left|z-s\right|\xi}\right],$$

$$\gamma_2^{hs}\left(\xi,z;s\right)=\frac{e^{-\left(s+z\right)\xi}+e^{-\left|z-s\right|\xi}}{2\xi},\qquad(28)$$

$$\gamma_3^{hs}\left(\xi,z;s\right)=\frac{1}{8\xi\left(1-\nu\right)}\left[\left(4-12\nu+8\nu^2+\left(3-4\nu\right)\xi\left(s-z\right)-2sz\xi^2\right)e^{-\left(s+z\right)\xi}+\left(s-z\right)e^{-\left|z-s\right|\xi}\right],$$

$$\Omega_1^{hs}\left(\xi,z;s\right)=\frac{1}{8\xi\left(1-\nu\right)}\left[\left(4-12\nu+8\nu^2+\left(3-4\nu\right)\xi\left(z-s\right)-2sz\xi^2\right)e^{-(s+z)\xi}+\left(z-s\right)e^{-|z-s|\xi}\right],$$

$$\Omega_2^{hs}\left(\xi,z;s\right)=\frac{1}{8\xi\left(1-\nu\right)}\left[\left(5-12\nu+8\nu^2+\left(3-4\nu\right)\xi\left(s+z\right)+2sz\xi^2\right)e^{-(s+z)\xi}+\left(3-4\nu+\left|z-s\right|\xi\right)e^{-|z-s|\xi}\right],$$

which are identical to the solution of the homogeneous half-space problem [55].

Three famous problems in elastostatic can be restored here:

i) For a concentrated vertical force, R_0, $\left(X_m=Y_m=0\right)$, after some simplifications, the results of the Mindlin's problem [18] will be restored:

$$u_z=\frac{R_0}{4\pi\mu}\left(\frac{rz}{\left(r^2+z^2\right)^{\frac{3}{2}}}+\left(1-2\nu\right)\frac{\left(r^2+z^2\right)^{\frac{1}{2}}-z}{r\left(r^2+z^2\right)^{\frac{1}{2}}}\right),$$

$$u_r=-\frac{R_0\cos\theta}{\pi\mu}\left(\frac{2r^2+z^2}{\left(r^2+z^2\right)^{\frac{3}{2}}}+\left(1-2\nu\right)\frac{z\left(r^2+z^2\right)^{\frac{1}{2}}-z^2}{r^2\left(r^2+z^2\right)^{\frac{1}{2}}}\right), \tag{29}$$

$$u_\theta=-\frac{R_0\sin\theta}{\pi\mu}\left(\frac{1}{\left(r^2+z^2\right)^{\frac{1}{2}}}+\left(1-2\nu\right)\frac{\left(r^2+z^2\right)^{\frac{1}{2}}-z}{r\left(r^2+z^2\right)^{\frac{1}{2}}}\right).$$

ii) By letting $s\to 0$, and just for a tangential concentrated force, results of Boussinesq's and Cerruti's fundamental problems will be derived.

iii) By letting $s\to\infty$, and setting a new coordinate system origin at the loading plane, results of celebrated Kelvin's problem will be represented

$$\gamma_1^{fs}\left(\xi,z;s\right)=\frac{3-4\nu-\xi\left|z-s\right|}{8\xi\left(1-\nu\right)}e^{-|z-s|\xi},$$

$$\gamma_2^{fs}\left(\xi,z;s\right)=\frac{1}{2\xi}e^{-|z-s|\xi},$$

$$\gamma_3^{fs}\left(\xi,z;s\right)=\frac{s-z}{8\xi\left(1-\nu\right)}e^{-|z-s|\xi}, \tag{30}$$

$$\Omega_1^{fs}\left(\xi,z;s\right)=\frac{z-s}{8\xi\left(1-\nu\right)}e^{-|z-s|\xi},$$

$$\Omega_2^{fs}\left(\xi,z;s\right)=\frac{3-4\nu+\xi\left|z-s\right|}{8\xi\left(1-\nu\right)}e^{-\left|z-s\right|\xi},$$

which are in exact agreement with the results reported by Love [56].

3.3 Inextensible thin film

By approaching $\kappa\to\infty$, the problem relates to a surface stiffened half-space with axially rigid membrane. The associated kernel functions are given by

$$\gamma_1^{\infty}\left(\xi,z;s\right)=\frac{1}{8\xi\left(1-\nu\right)}\left[-\left(3-4\nu-\xi\left(s+z\right)\right)e^{-\left(s+z\right)\xi}+\left(3-4\nu-\xi\left|z-s\right|\right)e^{-\left|z-s\right|\xi}\right],$$

$$\gamma_2^{\infty}\left(\xi,z;s\right)=-\frac{1}{2\xi}\left[e^{-\left(s+z\right)\xi}-e^{-\left|z-s\right|\xi}\right],$$

$$\gamma_3^{\infty}\left(\xi,z;s\right)=\frac{1}{8\left(1-\nu\right)}\left[-\left(s+z\right)e^{-\left(s+z\right)\xi}+\left(s-z\right)e^{-\left|z-s\right|\xi}\right],$$

$$\Omega_1^{\infty}\left(\xi,z;s\right)=\frac{1}{8\left(1-\nu\right)}\left[-\left(s+z\right)e^{-\left(s+z\right)\xi}+\left(z-s\right)e^{-\left|z-s\right|\xi}\right], \tag{31}$$

$$\Omega_2^{\infty}\left(\xi,z;s\right)=\frac{1}{8\xi\left(1-\nu\right)}\left[\left(3-4\nu+\xi\left(s+z\right)\right)e^{-\left(s+z\right)\xi}+\left(3-4\nu+\xi\left|z-s\right|\right)e^{-\left|z-s\right|\xi}\right].$$

$$\Omega_2^{\infty}(\xi,z;s)=\frac{1}{8\xi(1-\nu)}\left[(3-4\nu+\xi(s+z))e^{-(s+z)\xi}+(3-4\nu+\xi|z-s|)e^{-|z-s|\xi}\right].$$

3.4 Numerical results for specific source distribution

Having the expressions for the displacement and stress fields given in Eqs. (22) and (23), it is possible to discuss some natures of the problem under consideration. The coated half-space is subjected to a uniform circular patch load of radius a and total resultant $\mathcal{F}_v$ and $\mathcal{F}_h$ at depth $s=2a$ in z and r axis directions, respectively. It is assumed that in inclined cases of loading the vertical and horizontal components of the resultant buried source are equal ($\mathcal{F}_v=\mathcal{F}_h=\mathcal{F}/\sqrt{2}$). By using data for Aluminum material properties [57] such that $\mu=76$ GPa, $\nu=0.21$, and with assuming $\nu^F=0.3$, the normal displacement, $\pi a\mu\, u_z/\mathcal{F}$, (at $r=0.5a,\ \theta=0$) along the dimensionless z-axis, z/a, are plotted in Fig. 1 for various values of the normalized rigidity factors $\bar{\kappa}=\kappa/\mu a$. It is worth noting that to avoid symmetric effects and pertinent

simplifications, results will be presented along the axis $r = 0.5a$ instead of $r = 0$ (z-axis). The peak normal displacement happens at $z = 2a$. This maximum value rises as the rigidity of the membrane decreases, causing all graphs to approach the classic problem, $\kappa = 0$, studied by Guzina and Pak [15]. As shown in Fig. 2, an increase in the rigidity of the thin film enhances the stiffness of the coated half-space. Additionally, it is clear from the regularity conditions that mechanical fields vanish at distant points from the loading plane.

To provide a more in-depth explanation under an oblique load, Fig. 2 illustrates the same normal displacement component, similar to Fig. 1, but normalized with respect to the response of classic half-space without any reinforcement. As expected from the physics of the problem, for smaller values of the thin film's rigidity, κ, the normalized graph Fig. 2 tends to one; ie identical amounts for displacement and furthermore, for deeper points of the thin film, the solution of mechanical fields of surface stiffened half-space approaches to classical one. If the system under consideration is reinforced by an inextensible membrane ($\kappa \to \infty$) the maximum normal displacement around $r = z = 0.5a$ is reduced by 25% approximately.

Fig. 3 and Fig. 4 show dimensionless normal displacement along the surface of half-space for different rigidity values of the thin film in vertical and horizontal patch load cases separately and respectively. It is evident from Fig. 3 and the asymmetrical concept of the problem under horizontal forces that the origin point of the coordinate system will be fixed without any movement in the z direction; And the maximum normal displacement appears a little before the $r = 2a$. An interesting point to note in this graph is that, although the shear modulus, μ^F, becomes larger and larger, the thickness of the surface layer becomes smaller and smaller. As a result, the stiffness of that thin layer will remain constant, whereas one would expect a rigid layer at the surface with zero displacement when the shear modulus grows independently to infinity. This case, $\kappa \to \infty$, has more of a mathematical aspect, as it is based on limiting of the result of two simultaneous limitations on the shear modulus and the thickness of the thin layer. Furthermore, considering the approximation of the assumption of plane stress state, it has a high level of complexity.

The result associated with the axisymmetric part of elastic response due to uniform vertical patch load is in exact agreement with those reported by Ahmadi et al. [45]. This accordance is shown in Fig. 4 for $\kappa = 1$ and $\kappa \to \infty$ where the plotted graphs with markers correspond to the findings in reference [45] with matching rigidity values. Moreover, as depicted in Fig. 4, the maximum normal displacement for vertical loads occurs at $r = 0$.

To have a better insight into the effects of the surface reinforcement, dimensionless radial displacement component u_r is plotted versus *z*-axis along $r = a$ for uniform vertical load in Fig. 5, for uniform horizontal load in Fig. 6, and their superposition, uniform inclined load, in Fig. 7. The main amounts of radial displacement in Fig. 7 originate from the horizontal component of loading and, consequently, Fig. 6 outweighs the behavior of the ascribed system. According to the observations in Fig. 7, the larger amounts of radial displacement with smaller values of rigidity of the reinforcing film make sense physically and as anticipated, the highest levels of radial displacement occurred near the loading area.

It is evident in Fig. 5 that for rigid membranes, the radial displacement at the surface is zero, and the maximum value appears near the loading zone, causing the direction of the radial displacement vector to change around the loading plane, $z = 2a$.

The next numerical result is presented to demonstrate the effect of the thin film's action on the shear stress component σ_{zr} along the surface of coated half-space. Normalized shear stress component variations ($\pi a^2 \, \sigma_{zr}/\mathcal{F}$) versus r for inclined load and also for various values of rigidity (κ), belonging to the thin film are displayed in Fig. 8. As it is evident from this graph, for $\kappa = 0$ the amount of shear stress at the surface, $z = 0$, yields to zero that is called *traction free conditions*; On the other hand, the maximum amount of σ_{zr} for any value of rigidity, κ, takes place at $r = 0$.

4. Conclusion

In the present study, by virtue of displacement potential functions and integral transform methods, an isotropic surface stiffened half-space by an isotropic extremely thin membrane under arbitrary static buried loads has been analytically investigated. The derived equations as thin membrane surface effects are concluded under considerations of plane stress for linear elastic membrane and perfect bonding between the membrane and surrounding media with no sliding at boundaries:

$$\left(\frac{\kappa}{2\left(1+\nu^{F}\right)}\xi^{2} - \mu\frac{\partial}{\partial z} \right)\tilde{\psi}_{m}^{m^{I}} = 0,$$

$$\left(\nu\frac{\partial^{2}}{\partial z^{2}} - \frac{\kappa\xi^{2}}{2\mu\left(1+\nu^{F}\right)\left(1-\nu^{F}\right)}\frac{\partial}{\partial z} + \left(1-\nu\right)\xi^{2} \right)\tilde{\phi}_{m}^{m^{I}} = 0\,.$$

Explicit expressions for mechanical field components for an axisymmetric case of loads are derived. Owing to eliminating unknown constants belonging to the thin film layer, the proposed surface conditions provide a more convenient procedure than the 3D elasticity approach while high accuracy is preserved.

The generality and efficiency of the presented equations are illustrated through specific cases and comparative results deduced from numerical examples. According to the studied numerical examples of circular uniform loads, the following conclusions are drawn:

- Under the inclined loading, surface covered membrane reduces the normal displacement up to 25%, approximately, when $\kappa \to \infty$ in comparison with classic similar problem.
- Thin membrane effect on radial displacement behavior is more important. Individually for horizontal loads, so that the orientation of the radial displacement for elements located under and above of the loading depth, *s*, changes in the *z*-direction.
- Because of extremely thin covering film role, traction free conditions at the surface of half-space are not hold and stress components

$\sigma_{zr}(r,\theta,z=0)$ and $\sigma_{z\theta}(r,\theta,z=0)$ are not zero at the surface unless the rigidity, κ, tends to zero.

References

1. Greene, J.E. "Review Article: Tracing the recorded history of thin-film sputter deposition: From the 1800s to 2017", *Journal of Vacuum Science & Technology A*, **35**(5), pp. 05c204 (2017). DOI: 10.1116/1.4998940
2. Shadravan, A., Amani, M., and Jantrania, A. "Feasibility of thin film nanocomposite membranes for clean energy using pressure retarded osmosis and reverse electrodialysis", *Energy Nexus*, **7**, pp. 100141 (2022). DOI: 10.1016/j.nexus.2022.100141
3. Yang, L., Zhang, X., Rahmatinejad, J., et al. "Triethanolamine-based zwitterionic polyester thin-film composite nanofiltration membrane with excellent fouling-resistance for effective dye and antibiotic separation", *Journal of Membrane Science*, **670**, pp. 121355 (2023). DOI: 10.1016/j.memsci.2023.121355
4. Angell, J., Baumgartl, S., Beusse, R., et al. "Combined application of modern techniques for microares analysis on metallic coated steel sheet", *Steel Research International*, **69**(12), pp. 463-524 (1998). DOI: 10.1002/srin.199805585
5. Rajan, S.T., Subramanian, B., and Arockiarajan, A. "A comprehensive review on biocompatible thin films for biomedical application", *Ceramics International*, **48**(4), pp. 4377-4400 (2022). DOI: 10.1016/j.ceramint.2021.10.243
6. Arbani, M., Jamshidi, R., and Sadeghnejad, M. "Using of 2D element modeling to predict the glasphalt mixture rutting behavior", *Construction and Building Materials*, **68**, pp. 183-191 (2014). DOI: 10.1016/j.conbuildmat.2014.06.057
7. Ziari, H., Behbahani, H., Kamboozia, N., et al. "New achievements on positive effects of nanotechnology zyco-soil on rutting resistance and stiffness modulus of glasphalt mix", *Construction and Building Materials*, **101**, pp. 752-760 (2015). DOI: 10.1016/j.conbuildmat.2015.10.150

8. Shirazi, S.G., Valipourian, K., and Golhashem, M.R. "A review on geomembrane characteristics and application in geotechnical engineering", *International Journal of Civil and Environmental Engineering*, **13**(8), pp. 494-501 (2019). DOI number: 10.5281/zenodo.3455659

9. Rajesh, S., Choudhary, K., and Chandra, S. A. "Generalized model for geosynthetic reinforced railway tracks resting on soft clays", *International Journal for Numerical and Analytical Methods Geomechanics*, **39**(3), pp. 310-326 (2014). DOI: 10.1002/nag.2318

10. Oyegbile, B.O., and Oyegbile, B.A. "Applications of Geosynthetic Membranes in Soil Stabilization and Coastal Defense Structures", *International Journal of Sustainable Built Environment*, **6**(2), pp. 143-159 (2017). DOI: 10.1016/j.ijsbe.2017.04.001

11. Bourdeau, P.L. "Modeling of membrane action in a two-layer reinforced soil system", *Computers and Geotecnics*, **7**(2), pp. 19-36 (1989). DOI: 10.1016/0266-352X(89)90004-9

12. Gurtin, M.E., and Murdoch, A.I. "A continuum theory of elastic material surface", *Archive for Rational Mechanics and Analysis*, **14**, pp. 291-323 (1975). DOI: 10.1007/BF00261375

13. Cheng, W., Wang, J., Ma, X., et al. "A review on microstructures and mechanical properties of protective nano-multilayered films or coatings", *Journal of Material Research and Technology*, **27**, pp. 2413-2442 (2023). DOI: 10.1016/j.jmrt.2023.10.012

14. Altenbach, H., and Morozov, N.F. "Surface effects in solid mechanics: models, simulations and applications", 1st Ed., pp. 1-32, *Springer Berlin*, Heidelberg (2013). DOI:10.1007/978-3-642-35783-1

15. Guzina, B.B., and Pak, R.Y.S. "Static fundamental solutions for a bi-material full-space", *International Journal of Solids and Structures*, **36**(4), pp. 493-516 (1999). DOI: 10.1016/S0020-7683(98)00035-3

16. Liew, K.M., Liang, J., Ding, H.J., et al. "Elastic fields in two-joined half-spaces subject to point force and uniform ring loads", *Computers Methods in Applied Mechanics and Engineering*, **190**(29), pp. 3749-3769 (2001). DOI: 10.1016/S0045-7825(00)00293-0

17. Vijayakumar, S., and Cormack, D.E. "Greens functions for the biharmonic equation: bonded elastic media", *SIAM Journal on Applied Mathematics*, **47**(5), pp. 982-997 (1987). DOI: 10.1137/0147065

18. Mindlin, R.D. "Force at a point in the interior of a semi-infinite solid", *Physics*, **7**(5), pp. 195-202 (1936). DOI: 10.1063/1.1745385

19. Xiao, S., Yue, W.V., and Yue, Z.Q. “Extended Mindlin solution for a point load in transversely isotropic halfspace with depth heterogeneity”, *Engineering Analysis with Boundary Elements*, **150**, pp. 219-236 (2023). DOI: 10.1016/j.enganabound.2023.02.009

20. Pan, E., and Yuan, F.G. “Three-dimensional Greens functions in anisotropic bimaterials”, *International Journal of Solids and Structures*, **37**(38), pp. 5329-5351 (2000). DOI: 10.1016/S0020-7683(99)00216-4

21. Pan, E., and Yuan, F.G. “Three-dimensional Greens functions in anisotropic piezoelectric biomaterials”, *International Journal of Engineering Science*, **38**(17), pp. 1939-1960 (2000). DOI: 10.1016/S0020-7225(00)00017-3

22. Khojasteh, A., Rahimian, M., and Pak, R.Y.S. “Three-dimensional dynamic Greens functions in transversely isotropic bi-materials”, *International Journal of Solids and Structures*, **45**(18), pp. 4952-4972 (2008). DOI: 10.1016/j.ijsolstr.2008.04.024

23. Shodja, H.M., and Eskandari, M. “Axisymmetric time-harmonic response of a transversely isotropic substrate–coating system”, *International Journal of Engineering Science*, **45**, pp. 272-287 (2007). DOI: 10.1016/j.ijengsci.2006.11.001

24. Tian, R., Nie, G., Liu, J., et al. “On Rayleigh waves in a piezoelectric semiconductor thin film over an elastic half-space”, *International Journal of Mechanical Science*, **204**, pp. 106565 (2021). DOI: 10.1016/j.ijmecsci.2021.106565

25. Eskandari-Ghadi, M., Sture, S., Pak, R.Y.S., et al. “A tri-material elastodynamic solution for a transversely isotropic full-space”, *International Journal of Solids and Structures*, **46**(5), pp. 1121-1133 (2009). DOI: 10.1016/j.ijsolstr.2008.10.026

26. Song, W., Zou, D., Liu, T., et al. “Dynamic response of unsaturated full-space caused by a circular tunnel subjected to a vertical harmonic point load”, *Soil Dynamics and Earthquake Engineering*, **130**, pp. 106005 (2020). DOI: 10.1016/j.soildyn.2019.106005

27. Yuan, Z., Bostrom, A., Cai, Y., et al. “Analytical wave function method for modelling a twin tunnel embedded in a saturated poroelastic full-space”, *Computers and Geotechnics*, **114**, pp. 103114 (2019). DOI: 10.1016/j.compgeo.2019.103114

28. Eskandari, M., and Shodja, H.M. “Green’s functions of an exponentially graded transversely isotropic half-space”, *International Journal of Solids*

and Structures, **47**(11-12), pp. 1537-1545 (2010). DOI: 10.1016/j.ijsolstr.2010.02.014

29. Oestringer, L.J., and Proppe, C. "On the fully coupled quasi-static equations for the thermoelastic halfspace", *Mechanics of Materials*, **177**, pp. 104554 (2023). DOI: 10.1016/j.mechmat.2022.104554

30. Selvadurai, A.P.S., and Samea, P. "Mechanics of a pressurized penny-shaped crack in a poroelastic halfspace", *International Journal of Engineering Science*, **163**, pp. 103472 (2021). DOI: 10.1016/j.ijengsci.2021.103472

31. Selvadurai, A.P.S., and Samea, P. "On the indentation of a poroelastic halfspace", *International Journal of Engineering Science*, **149**, pp. 103246 (2020). DOI: 10.1016/j.ijengsci.2020.103246

32. Xiao, S., and Yue, Z.Q. "Axisymmetric BEM analysis of one-layered transversely isotropic halfspace with cavity subject to external loads", *Engineering Analysis with Boundary Elements*, **121**, pp. 91-103 (2020). DOI: 10.1016/j.enganabound.2020.09.006

33. Xiao, S., and Yue, Z.Q. "Axisymmetric BEM analysis of layered elastic halfspace with volcano-shaped mantle and cavity under integral gas pressure", *Engineering Analysis with Boundary Elements*, **130**, pp. 404-416 (2021). DOI: 10.1016/j.enganabound.2021.06.003

34. Suo, Z., and Hutchinson, J.W. "Interface crack between two elastic layers", *International Journal of Fracture*, **43**(1), pp. 1-18 (1990). DOI: 10.1007/BF00018123

35. Qu, J., and Bassani, J.L. "Interfacial fracture mechanics for anisotropic biomaterials", *Journal of Applied Mechanics*, **60**(2), pp. 422-431 (1993). DOI: 10.1115/1.2900810

36. Selvadurai, A.P.S. "A unilateral contact problem for a rigid disc inclusion embedded between two dissimilar elastic half-spaces", *The Quarterly Journal of Mechanics and Applied Mathematics*, **47**(3), pp. 493-510 (1994). DOI: 10.1093/qjmam/47.3.493

37. Selvadurai, A.P.S. "An inclusion at a bi-material elastic interface", *Journal of Engineering Mathematics*, **37**(1), pp. 155-170 (2000). DOI: 10.1023/A:100478211071

38. Gladwell, G.M.L. "On inclusions at a bi-material elastic interface", *Journal of Elasticity*, **54**(1), pp. 27-41 (1999). DOI: 10.1023/A:1007616112455

39. Chen, W. “Surface effect on Bleustein-Gulyaev wave in a piezoelectric half-space”, *Theoretical and Applied Mechanics Letters,* **1**(4), pp. 041001 (2016). DOI: 10.1063/2.1104101

40. Lambros, J., and Rosakis, A.J. “Shear dominated transonic interfacial crack growth in a bimaterial- I: Experimental observations”, *Journal of the Mechanics and Physics of Solids,* **43**(2), pp. 169-188 (1995). DOI: 10.1016/0022-5096(94)00071-C

41. Wu, Z. “Experimental and numerical investigation of the interfacial strength of bi material joints”, *International Journal of Adhesion and Adhesives,* **77**, pp. 29-34 (2017). DOI: 10.1016/j.ijadhadh.2017.04.004

42. Benveniste, Y., and Miloh, T. “Imperfect soft and stiff interfaces in two-dimensional elasticity”, *Mechanics of Materials,* **33**(6), pp. 309-323 (2001). DOI: 10.1016/S0167-6636(01)00055-2

43. Benveniste, Y. “Models of thin interphases with variable moduli in plane-strain elasticity”, *Mathematics and Mechanics of Solids,* **18**(2), pp. 119-134 (2013). DOI: 10.1177/1081286512462186

44. Zafari, Y., Shahmohamadi, M., Khojasteh, A., et al. “Three-dimensional axisymmetric responses of exponentially graded transversely isotropic tri-materials under interfacial loading”, *Scientia Iranica,* **24**(3), pp. 966-978 (2017). DOI: 10.24200/sci.2017.4080

45. Ahmadi, S.F., Samea, P., and Eskandari, M. “Axisymmetric response of a bi-material full-space reinforced by an interfacial thin film”, *International Journal of Solids and Structures,* **90**, pp. 251-260 (2016). DOI: 10.1016/j.ijsolstr.2016.02.011

46. Kalantari, M., Khojasteh, A., Mohammadnezhad, H., et al. “An inextensible membrane at the interface of a transversely isotropic bi-material full-space”, *International Journal of Engineering Science,* **91**, pp. 34-48 (2015). DOI: 10.1016/j.ijengsci.2015.02.004

47. Rahman, M., and Newaz, G. “Elastostatic surface displacement of a half-space reinforced by a thin film due to an axial ring load”, *International Journal of Engineering Science,* **35**(6), pp. 603-611 (1997). DOI: 10.1016/S0020-7225(96)00096-1

48. Ahmadi, S.F., and Eskandari, M. “Axisymmetric circular indentation of a half-space reinforced by a buried elastic thin film”, *Mathematics and Mechanics of Solids,* **19** (6), pp. 703-712 (2014). DOI: 10.1177/1081286513485085

49. Selvadurai, A.P.S. “Boussinesq indentation of an isotropic elastic half-space reinforced with an inextensible membrane”, *International Journal*

of Engineering Science, **47**(11-12), pp. 1339-1345 (2009). DOI: 10.1016/j.ijengsci.2008.08.004

50. Eskandari, M., Samea, P., and Ahmadi, S.F. "Axisymmetric time-harmonic response of a surface-stiffened transversely isotropic half-space", *Meccanica*, **52** (1-2), pp. 183-196 (2017). DOI: 10.1007/s11012-016-0387-1

51. Bagheri, A., Khojasteh, A., Rahimian, M., et al. "Dispersion of surface waves in a transversely isotropic half-space underlying a liquid layer", *Scientia Iranica*, **23**(6), pp. 2469-2477 (2016). DOI: 10.24200/sci.2016.2306

52. Ahmadi, K.A.K, Jarfi, H., and Eskandari, M. "Elastic responses of bi-material media reinforced by interfacial thin films under asymmetric loading", *International Journal of Solids and Structures*, **254-255**, pp. 111928 (2022). DOI: 10.1016/j.ijsolstr.2022.111928

53. Sadd, M.H. "Elasticity: theory, applications, and numeric", *Elsevier Academic Press*, 3rd Edn., pp. 66-70, Amsterdam, Netherlands (2014). DOI: 10.1016/B978-0-12-408136-9.01001-1

54. Muki, R. "Asymmetric problems of the theory of elasticity for a semi-infinite solid and a thick plate", *In Progress in Solid Mechanics*, I. N. Sneddon, and R. Hill, Ed., Vol. 1, pp. 399-439, North-Holland publication company, Amsterdam (1960).

55. Saphores, J.D.M. "Some topics in embedded foundations", M.S. thesis University of Colorado, Boulder, USA (1989).

56. Love, A.E.H. "A Treatise on the Mathematical Theory of Elasticity", *Dover Books on Engineering Series*, 2nd Edn., pp. 236-253, Cambridge University Press, pp. 236-253, Cambridge, UK (1906).

57. Meyers, M.A., and Chawla, K.K. "Mechanical Behavior of Materials", Vol. 2, 2nd Edn., pp. 420-425, *Cambridge University Press*, Cambridge (2008). DOI: 10.1017/CBO9780511810947

List of figure captions:

Fig. 1. Normal displacement along the z-axis of a coated half-space under circular inclined patch load of radius a and total resultant $\mathcal{F}$ for various values of rigidity, κ.

Fig. 2. Normalized displacement ratio along the z-axis of a coated half-space under circular inclined uniform patch load of radius a and total resultant $\mathcal{F}$.

Fig. 3. Normal displacement along the r-axis of a coated half-space under circular horizontal uniform patch load of radius a and total resultant $\mathcal{F}_{\mathrm{h}}$.

Fig. 4. Normal displacement along the r-axis of a coated half-space under circular vertical uniform patch load of radius a and total resultant $\mathcal{F}_{\mathrm{v}}$.

Fig. 5. Radial displacement along the z-axis of a coated half-space under uniform circular vertical patch load of radius a and total resultant $\mathcal{F}_{\mathrm{v}}$.

Fig. 6. Radial displacement along the z-axis of a coated half-space under uniform circular horizontal patch load of radius a and total resultant $\mathcal{F}_{\mathrm{h}}$.

Fig. 7. Radial displacement along the z-axis of a coated half-space under uniform circular inclined patch load of radius a and total resultant $\mathcal{F}$.

Fig. 8. Shear stress component along the r-axis at the surface of a coated half-space under circular inclined uniform patch load of radius a and total resultant $\mathcal{F}$.

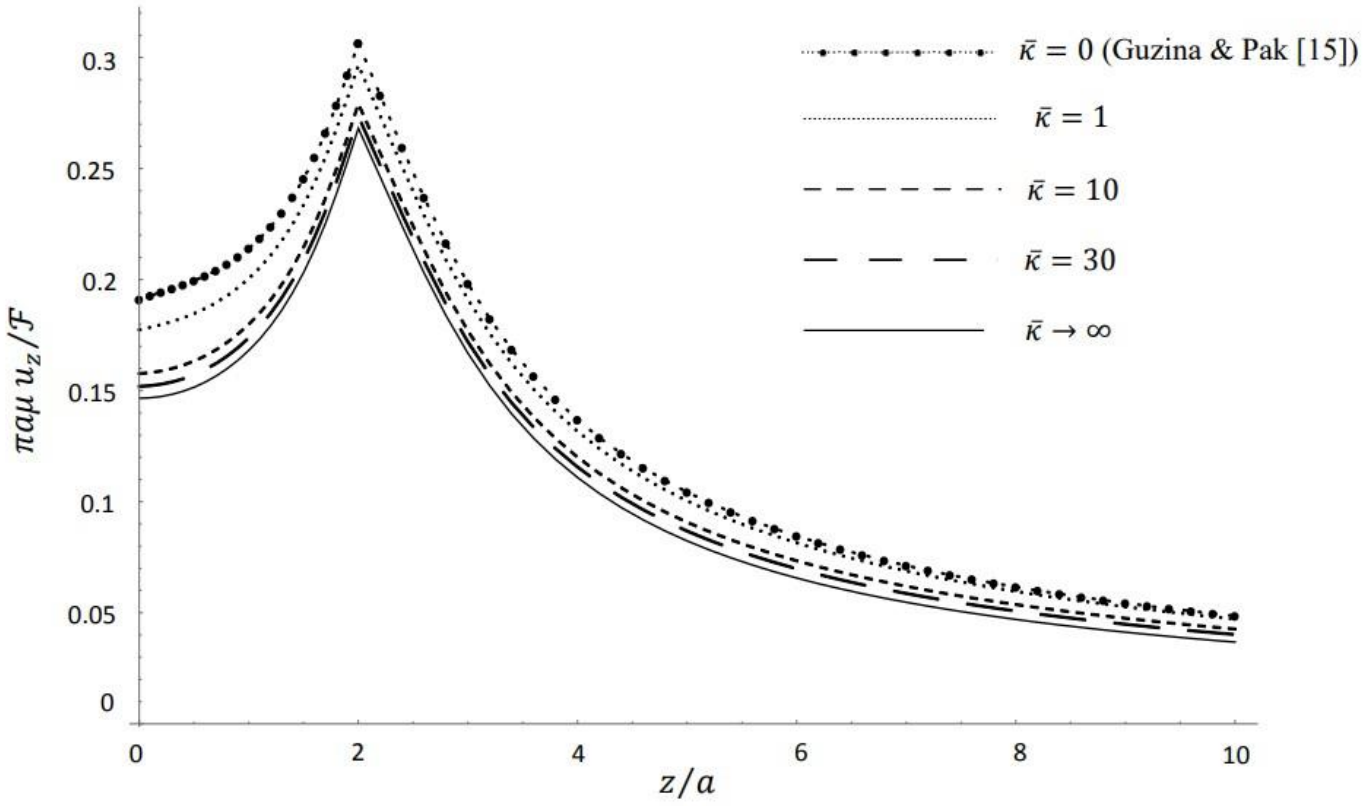

Fig. 1. *Normal displacement along the z-axis of a coated half-space under circular inclined patch load of radius a and total resultant F for various values of rigidity, κ.*

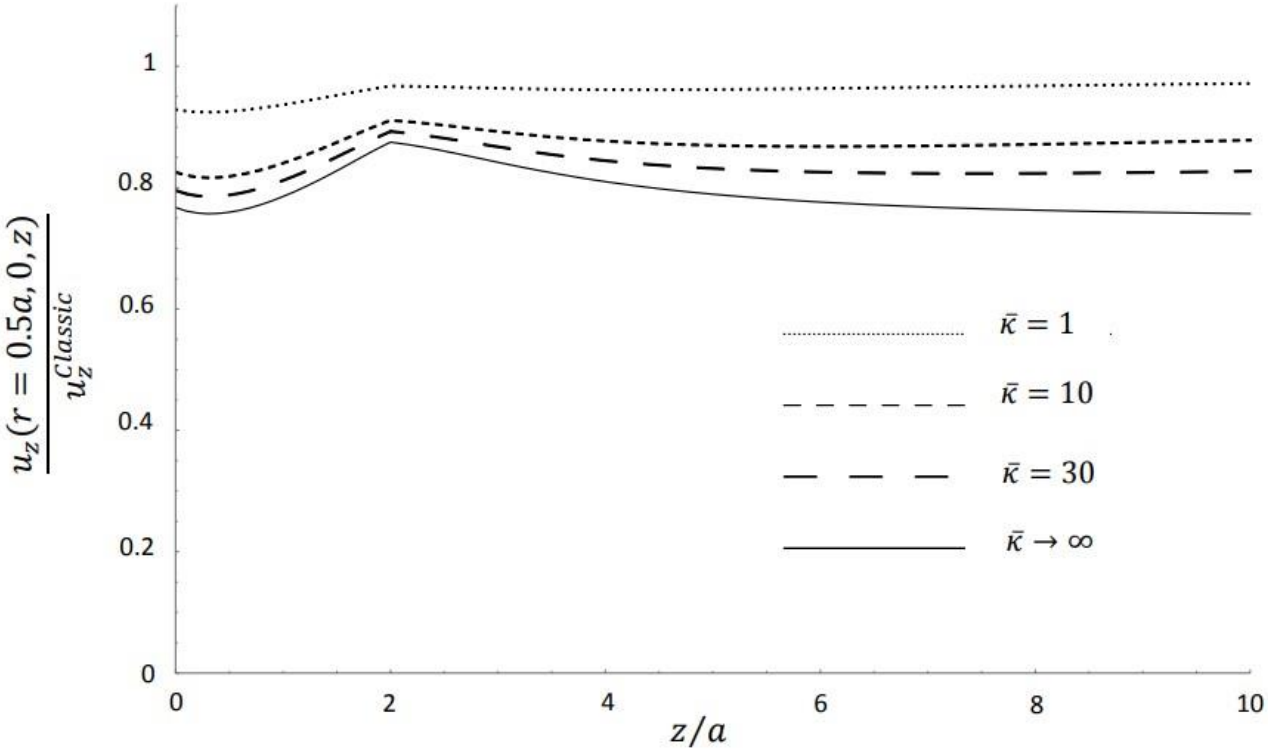

Fig. 2. *Normalized displacement ratio along the z-axis of a coated half-space under circular inclined uniform patch load of radius a and total resultant F.*

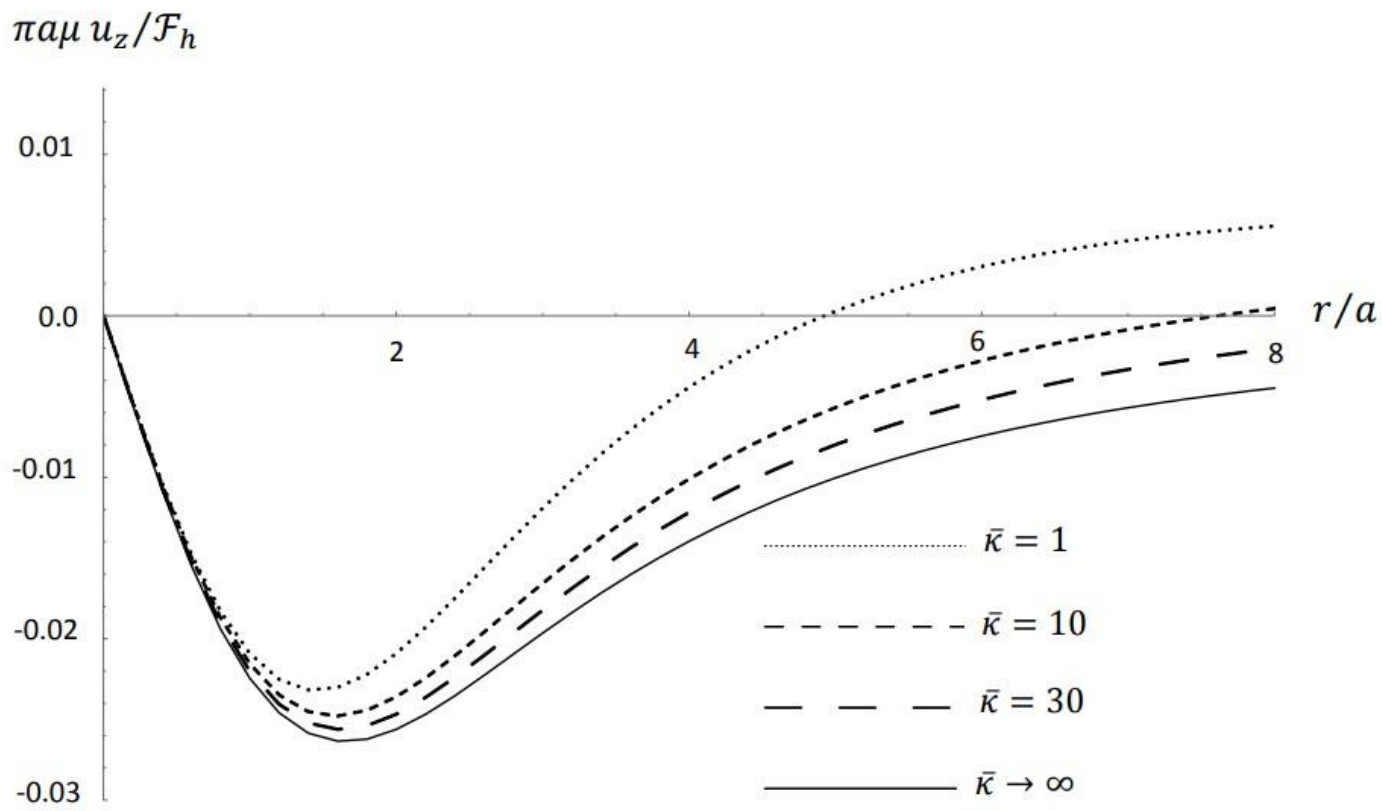

Fig. 3. *Normal displacement along the r-axis of a coated half-space under circular horizontal uniform patch load of radius a and total resultant F_h.*

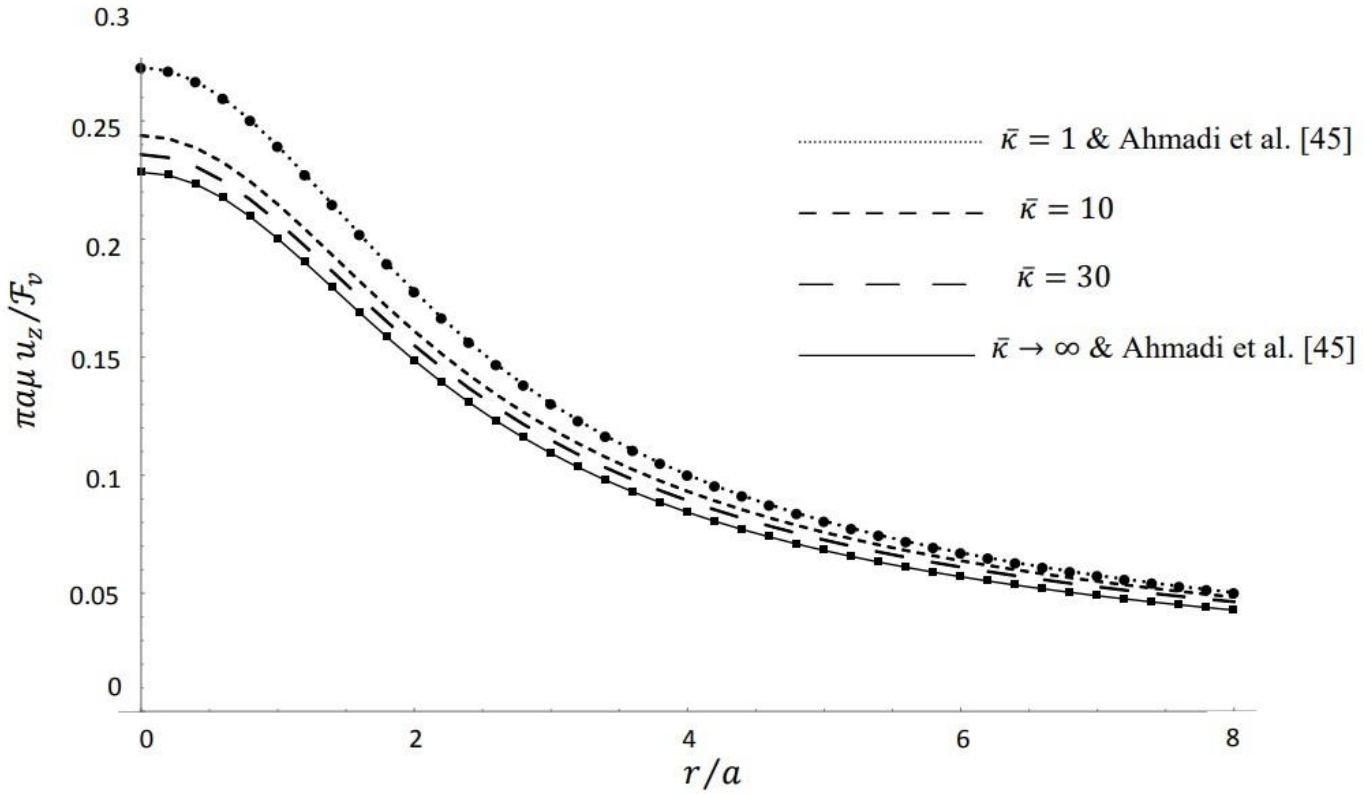

Fig. 4. *Normal displacement along the r-axis of a coated half-space under circular vertical uniform patch load of radius a and total resultant F_v.*

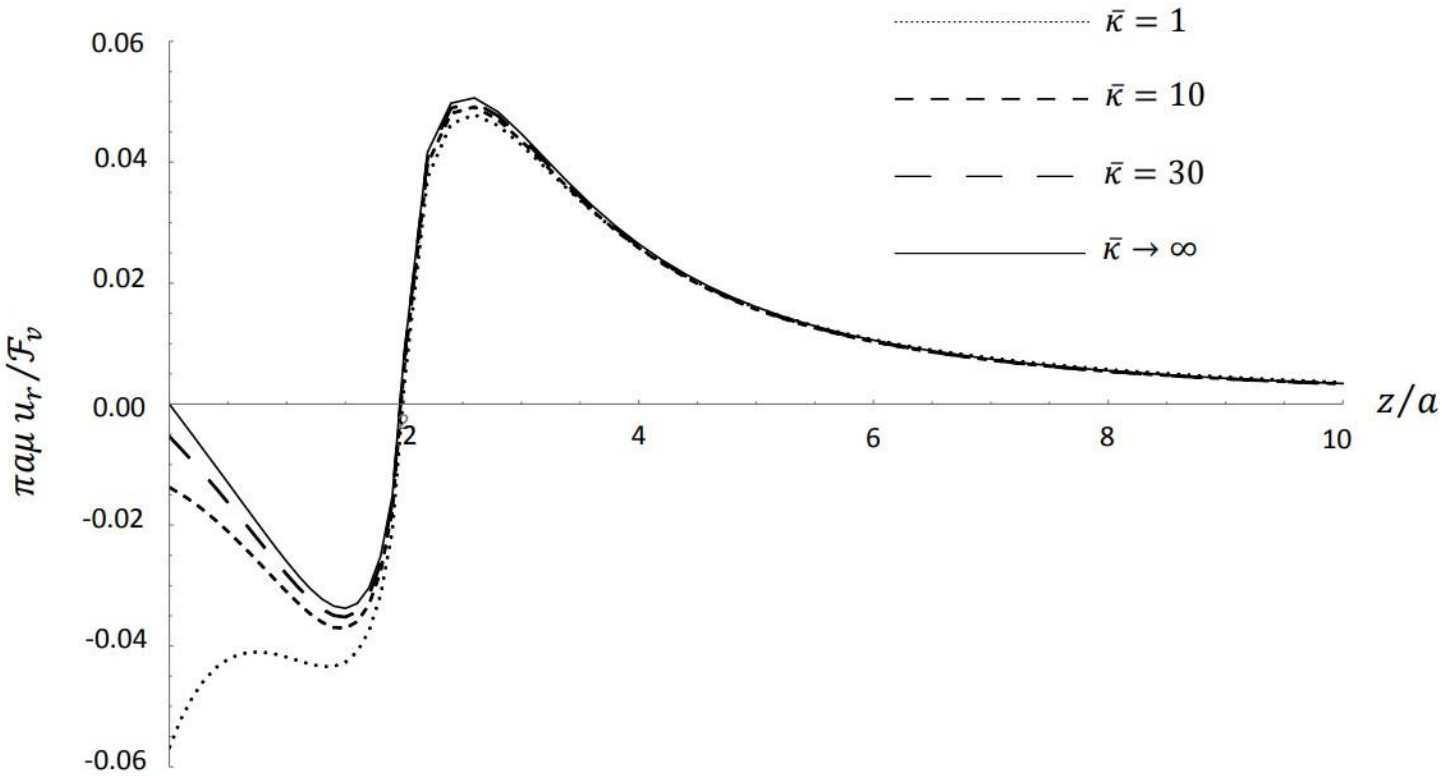

Fig. 5. *Radial displacement along the z-axis of a coated half-space under uniform circular vertical patch load of radius a and total resultant F_v.*

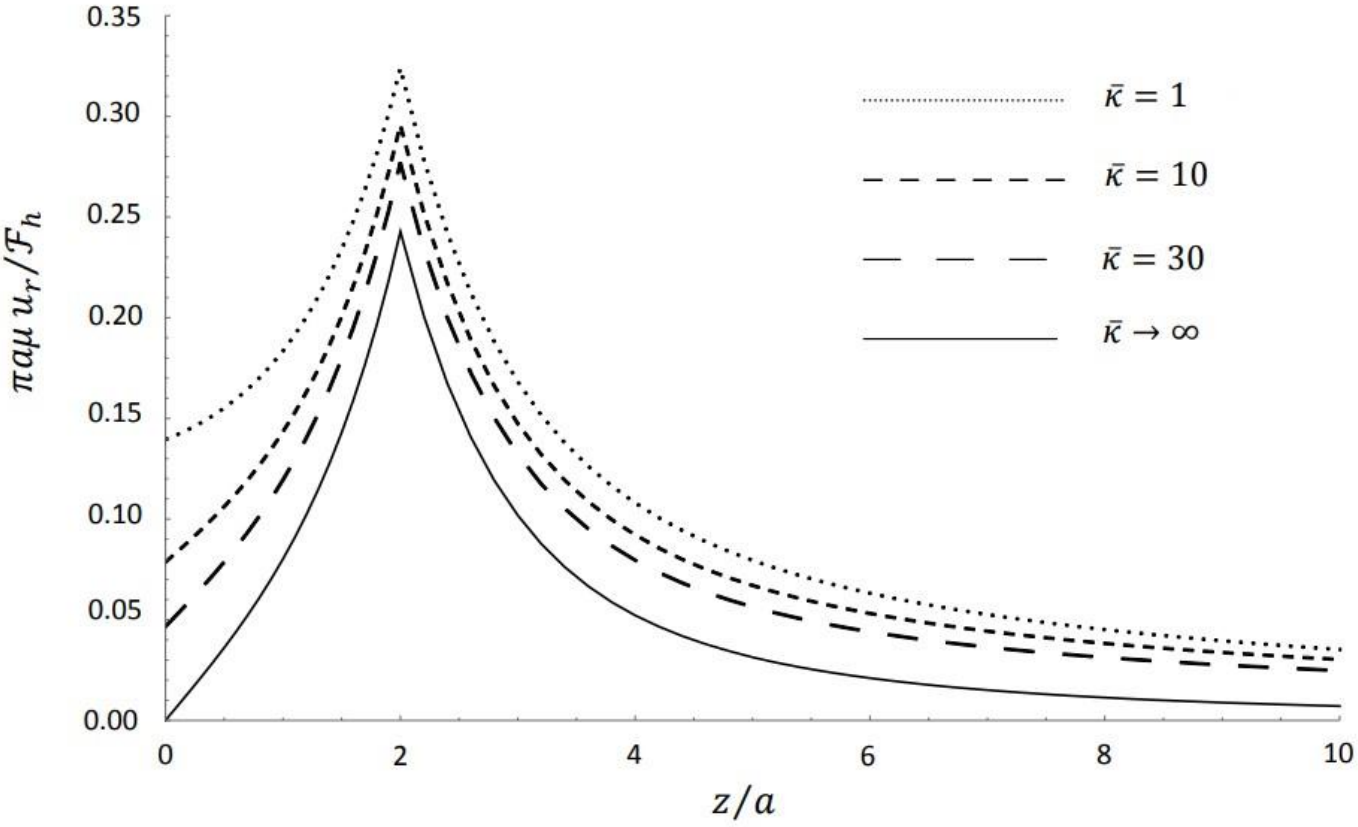

Fig. 6. *Radial displacement along the z-axis of a coated half-space under uniform circular horizontal patch load of radius a and total resultant F_h.*

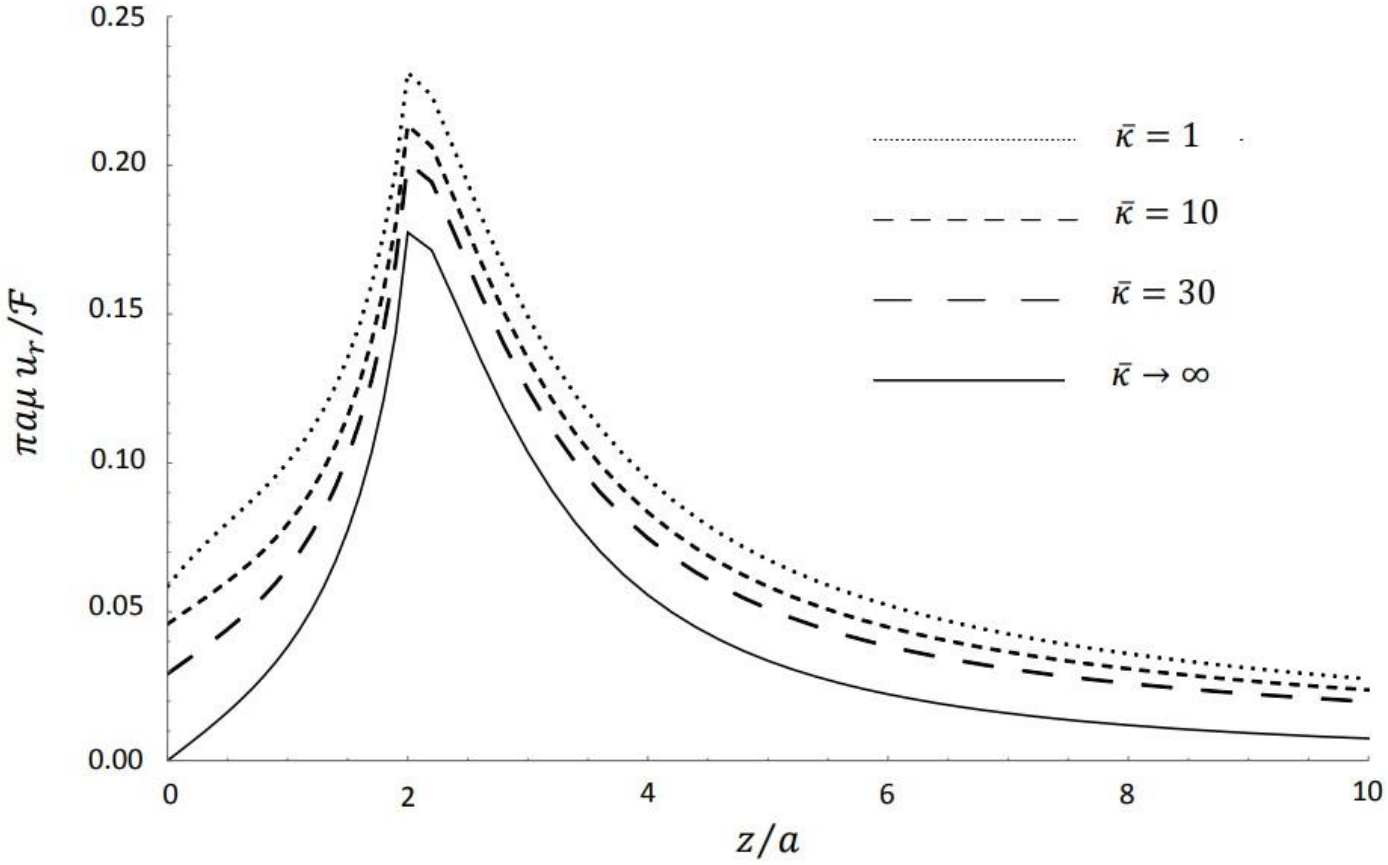

Fig. 7. *Radial displacement along the z-axis of a coated half-space under uniform circular inclined patch load of radius a and total resultant F.*

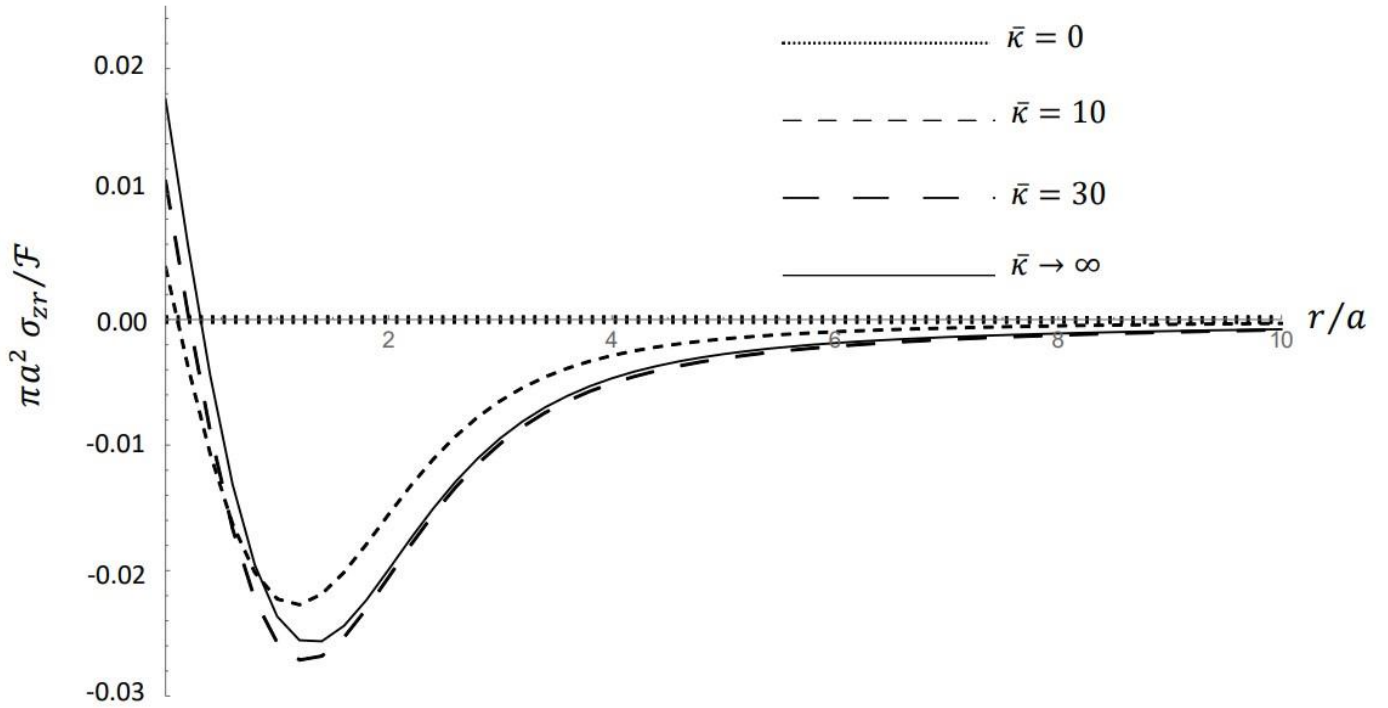

Fig. 8. *Shear stress component along the r-axis at the surface of a coated half-space under circular inclined uniform patch load of radius a and total resultant F.*